Zinc Oxide Nanoparticles Made with *Phyla nodiflora* Leaf Extract Have Anti-Hyperuricemic Effect on Monosodium Urate Crystal-induced Gouty Arthritis

Xianyao Li,[a] Yaqin Tang,[b] and Lihua Li [c,*]

*****Corresponding author: lilihua0328@163.com

DOI: 10.15376/biores.19.4.9544-9559

GRAPHICAL ABSTRACT

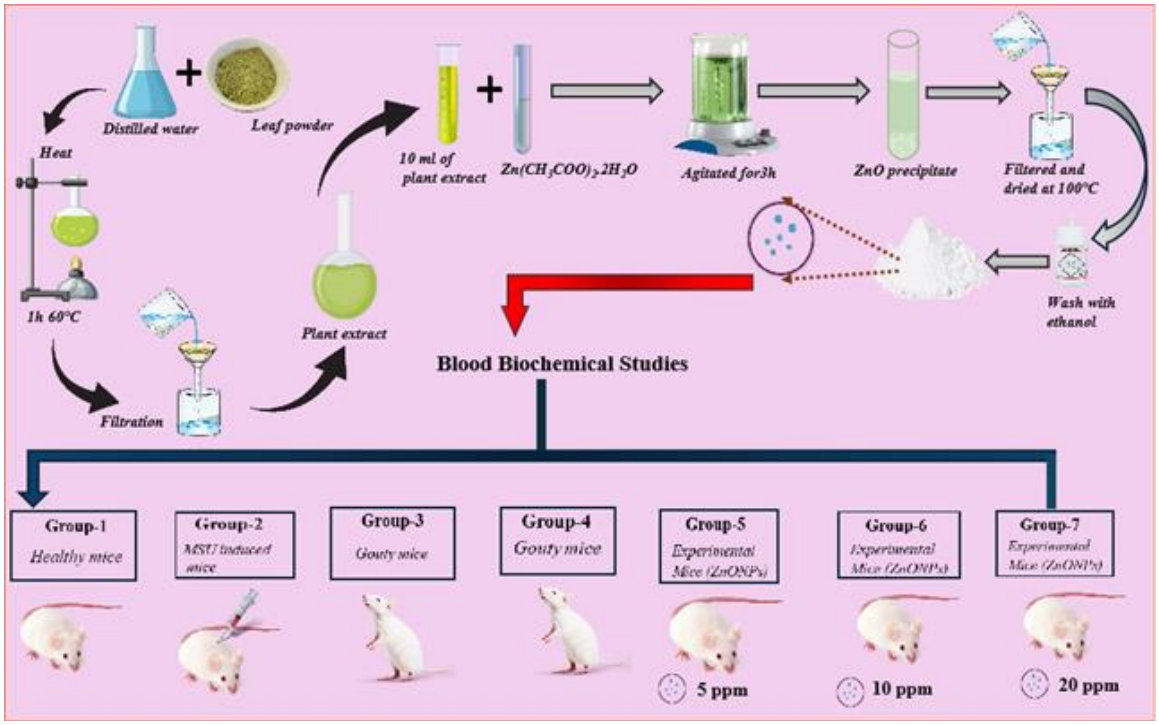

Zinc Oxide Nanoparticles Made with *Phyla nodiflora* Leaf Extract Have Anti-Hyperuricemic Effect on Monosodium Urate Crystal-induced Gouty Arthritis

Xianyao Li,[a] Yaqin Tang,[b] and Lihua Li [c,*]

The production of nanoparticles in the presence of biomaterials has become a promising substitute to traditional chemical and physical manufacturing procedures. Zinc oxide nanoparticles (ZnO-NPs) were prepared using *Phyla nodiflora* leaf extracts as a natural reducing agent, along with distilled water. The nanoparticles were analysed using various methods such as transmission electron microscopy, Fourier transformed infrared spectroscopy, UV-visible spectroscopy, energy dispersive X-ray, X-ray diffraction, dynamic light scattering, and zeta potential to examine their synthesis, structural morphology, chemical bonding, elemental composition, and crystalline structure. ZnO-NPs were orally provided for three weeks instead of usual drinking water to assess their therapeutic efficacy. Blood biochemical examinations were performed, including liver and kidney function tests, lipid profiles, and complete blood counts. The study exhibited a notable reduction in blood urea, creatinine, and uric acid levels, substantially alleviating hyperuricemia and gouty arthritis. A slight increase in liver enzymes, alkaline phosphatase (ALP), aspartate transaminase (AST), and alanine transaminase (ALT) was detected in the study groups, with no negative changes histopathologically found in the liver, muscle, or kidney tissues. The results indicate that ZnO-NPs have the potential to be an effective alternative to current pharmaceutical treatments for hyperuricemia and gouty arthritis.

DOI: 10.15376/biores.19.4.9544-9559

Keywords: ZnO-NPs; Hyperuricemia; Uric acid; Histology

*Contact information: a: Department of Rheumatology and Immunology, Changde Hospital, Xiangya School of Medicine, Central South University (The first people's hospital of Changde city), Changde 415000, Hunan, China; b: Department of Basic Medicine, School of Medicine, Yangzhou University, Yangzhou 225000, Jiangsu, China; c: Department of Science and Education, Changde Hospital, Xiangya School of Medicine, Central South University (The first people's hospital of Changde city), Changde 415000, Hunan, China; *Corresponding author: lilihua0328@163.com*

INTRODUCTION

Gouty arthritis is an inflammatory joint disorder that largely occurs due to urate crystals accumulation and activation of the innate immune system. This illness affects many people worldwide (Kuo *et al.* 2015). Elevated amounts of uric acid in the blood can result in severe gouty arthritis, uric acid kidney stones, and the development of joint tophi (Kim *et al.* 2022). Monosodium urate (MSU) crystals can cause severe pain by mechanically irritating adjacent synovial tissues during gout attacks (Ashiq *et al.* 2018). Recently, there has been a significant rise in the prevalence of gout, as well as other health concerns including diabetes, cardiovascular issues, and renal ailments (Richette *et al.* 2014; Zhang *et al.* 2016). Gout therapy includes using uricosurics to increase uric acid excretion

or inhibiting xanthine oxidase (XO) activity to decrease uric acid production (Elahi and Matata 2013; Susyani *et al.* 2017). Uric acid has a role in medicinal uses. The XO also plays a role in producing reactive oxygen species, which are linked to oxidative stress, ageing, cancer development, liver inflammation, and other inflammatory disorders (Bustanji *et al.* 2011; Elahi *et al.* 2013). Allopurinol, an XO inhibitor, is commonly used to treat gout but can cause adverse effects such as nephropathy, liver inflammation, and allergic responses (Sezai *et al.* 2015).

Metal oxide nanoparticles in biomedicine have demonstrated potential in treating cancer, microbial infections, and improving cell imaging (Singh *et al.* 2016). ZnO-NPs and other metal-based nanoparticles are known for their versatility in several uses, including as antibacterial agents, catalysts, and to combat antibiotic resistance. Distinct characteristics and methods of operation make nanoparticles extremely significant in research as well as possible clinical or industrial uses (Matei *et al.* 2008; Jones *et al.* 2011). Metal nanoparticle's capacity to interact with several biomolecular targets in bacteria decreases the chances of resistance development, providing a crucial benefit in combating drug-resistant bacterial strains (Zare *et al.* 2017; Sajid *et al* 2022 Foudi *et al.* 2023). Analyzing these metal-based nanoparticles using different analytical methods reveals details on their structure, physical, chemical, and electrical properties, which are essential for understanding their biological activity and developing safe and efficient uses in the fields of medicine and nanotechnology (Slavin *et al.* 2017; Wang *et al.* 2017; AI-Dhabi *et al.* 2018).

The present study investigated the effectiveness of biosynthesis and chemical precipitation procedures using *Phyla nodiflora*, which has been used in Ayurvedic and Siddha medicine to treat urinary issues, joint pain, and inflammation. The research on the plant's ability to combat hyperuricemia included studying its xanthine oxidase inhibition, uricosuric effects, and its ability to inhibit liver xanthine oxidase/xanthine dehydrogenase (XOD/XDH) activity in mice with hyperuricemia induced by MSU crystals. The eco-friendly synthesis of ZnO-NPs using *Phyla nodiflora* is notable for its capacity to reduce and stabilize the particles without the need of hazardous chemicals or risk of microbial contamination, making it cost-effective and environmentally benign. This is in line with the growing focus on sustainable nanotechnology practices (Hasan *et al.* 2019).

This study investigated the effects of orally ingested ZnO-NPs on gout in living organisms. The study involved using Balb/C mice to induce gout by administering MSU crystals. The mice were then treated with various amounts of ZnO-NPs. The study investigated the influence of ZnO-NPs on gout by thoroughly evaluating different biochemical parameters to measure the effectiveness of the nanoparticles.

EXPERIMENTAL

Materials and Methods

Collection and processing of plant materials

Phyla nodiflora, a medicinal plant, was obtained from the Botanical Garden of the Department of Botany at Sardar Bahadur Khan Women's University with the institution's agreement. The gathered plant material was washed with tap water and then rinsed with distilled water to remove dust, and subsequently air-dried to remove moisture. The desiccated leaves were pulverized into a fine powder. To produce the aqueous extract, 5 g

of the powder was heated in 100 mL of double-distilled water at 60 °C for 1 h, filtered using Whatman no. 1 filter paper, and stored at 4 °C.

Biosynthesis of ZnO-NPs

At first 0.02 M solution of zinc acetate dihydrate ($Zn(CH_3COO)_2 \cdot 2H_2O$) was prepared. Next, about 100 mL of double-distilled water was used to boil 5 g of finely powdered leaves at 60 °C for 1 h to prepare extract solution. To eliminate any residual particles, Whatman no. 1 filter paper was used to filter the extract, which was stored at 4 °C for future use. To prepare ZnO NPs, the as prepared zinc acetate dihydrate was added to 10 mL of the plant extract. The mixture was continuously stirred on a heating plate for 3 h at a moderate temperature using a magnetic stirrer, leading to the formation of white ZnO NP precipitates. The precipitates were presumably isolated through filtration and subsequently washed with distilled water several times to eliminate any remaining contaminants. Subsequently, the sample was rinsed with ethanol to improve its purity. To remove moisture, the NPs were dehydrated in an oven at 100 °C for 1 h.

Optimization of Physicochemical Parameters for ZnO NPs Biosynthesis

Effect of pH

The pH levels of reaction mixture were adjusted to 8.0, 10.0, 12.0, and 14.0 using a 2M NaOH solution. Throughout the experiment, the concentration of the reaction mixture, reaction time, and temperature were kept constant. Absorbance measurements were taken using a spectrophotometer. This process was repeated three times to optimize the pH conditions.

Effect of concentration of metal ion

The metal ion concentration was set at 0.005, 0.01, and 0.02 M, while the concentration of the plant extract, pH, temperature, and incubation time remained constant. Absorbance measurements were taken between 300 and 500 nm, following the procedure outlined earlier.

Effect of reaction time

The reaction mixture was maintained at room temperature at 1h, 2h, and 3h intervals to examine the impact of reaction time on the synthesis of NPs.

Effect of temperature

Temperature, a key physicochemical parameter, was controlled at 30, 60, and 90 °C using a water bath. Absorbance measurements were taken following the spectrophotometric method previously described by Jamdagni *et al.* (2016). The concentrations of metal ions, reaction time, and pH of the reaction mixture were kept constant throughout the experiment.

Characterization

The nanoparticles were characterized using various analytical methods. Fourier transform infrared (FTIR) spectroscopy (Nicolet 6700, Thermo Scientific, USA) detects chemical bonds and functional groups through the absorption of infrared radiation. Ultraviolet-visible (UV-Vis) spectrometry (Uviline 9400, Secomam, France) analysed the electrical structure of the nanoparticles and measured the concentration of species that absorb UV and visible light. Transmission electron microscopy (TEM) produces high

resolution surface pictures by transmitting a high-energy beam of electrons through the sample. Energy dispersive X-ray (EDX) (JEM-2100F, JEOL, Tokyo, Japan) analysis examines the elemental composition by studying the X-ray energy and intensity produced when electrons interact with the sample. The crystalline structure was analysed using X-ray diffraction (XRD) with Cu Kα radiation to study the diffraction patterns of X-rays dispersed by the crystalline lattice. Dynamic light scattering (DLS) (Nano S Malvern Instruments, UK), was used to analyze the hydrodynamic size and zeta potential of the prepared NPs.

Animals Research and Methodology

Forty-two Balb/C mice, weighing 25 to 30 g and of both genders were placed into seven groups, each group including six animals. Four groups were designated as controls, in which Group 1 contained healthy mice, Group 2 contained MSU-induced gouty mice with no treatment, Groups 3 and 4 contained gouty mice with orally administered allopurinol (50 and 100 mg/kg, respectively), whereas three groups were part of the experimental set, in which Groups 5, 6, and 7 contained gouty mice with orally administered ZnO-NPs (5, 10, and 20 ppm). The animals were kept in aired cages with a regular 12-h light/dark cycle. The surrounding temperature was maintained at 25 ± 1 °C with controlled humidity, and fluorescent lighting was used to mimic natural daylight. All mice were fed pellets containing 6 mg/kg of zinc in the form of zinc acetate, following known dietary standards, as detailed in Table 1. Gouty arthritis was produced in all mice in the control set, by administering MSU crystals except for the first group of normal mice. ZnO-NPs were synthesized at different concentrations (5, 10, and 20 ppm) by dissolving them in water and subjecting them to sonication to achieve even distribution. The nanoparticles were given to the mice orally for 21 days by substituting their usual drinking water with the nanoparticle solution (Razavian *et al.* 2014).

Table 1. The Dietary Composition Provided to Mice

Requirements	Growth Diet (g/kg Diet)	Adult Diet (g/kg Diet)
Casein (> 85% protein)	203.9	206.9
Sucrose	100.4	103
Corn starch	399.5	468.7
Soya bean oil	74.8	78
Dextrine Containing cornstarch	135.9	157.1
Vitamin mix	12.6	12.6
Mineral mix	37.6	37.6
Fibers	40	40
Choline bi-tartrate	3.2	3.2
Tert-butylhydroquinone	0.036	0.02
L-cysteine	5.2	2.2

Preparation and Application of MSU Crystals to Induce Gout

The MSU crystals were synthesized by combining uric acid with NaOH. The mixture was heated to 70 °C while maintaining the pH levels within the range of 7.1 to 7.2. Uric acid of 1.68 g was combined with 0.001 M NaOH solution and kept at room temperature for 24 h. Following this timeframe, the liquid portion was removed, and the crystals that remained were cleaned and dried multiple times (So *et al.* 2007). The mice

were induced with gout by receiving their initial intra-articular injection of MSU crystals into the left ankle once daily for three consecutive weeks. For the following two weeks, the mice received MSU crystals *via* intraperitoneal injections to maintain the induction process.

RESULTS AND DISCUSSION

Characterization

Table 2 shows the measured properties of the nanoparticles.

Table 2. Characterisation Results of ZnO NPs Prepared with *Phyla nodiflora* Plant Extract

Characterization technique	Parameter measured	Results
UV-Vis	Absorption of ultraviolet and visible light by nanoparticles	370 nm
FTIR	Functional groups	Peaks at 3330.9 cm^{-1}, 2130.5 cm^{-1}, 1630.7 cm^{-1}, and 528 cm^{-1}
XRD	Crystal structure	Hexagonal wurtzite
TEM	Size, shape	20-50 nm, spherical, hexagonal
DLS	Particle size distribution	38 nm
EDX	Elemental composition	Zinc and oxygen
DLS	Zeta potential	-30.3 mV

UV-Vis spectroscopy

Figure 1 displays the UV-visible absorption spectrum of ZnO-NPs, showing a noticeable shift towards the blue end with absorption peak at 370 nm. This peak was located in the UV spectrum between 200 and 400 nm, indicating the nanoparticle's strong absorbance capabilities. The distinct absorbance peaks at 370 nm are a strong indication of the exceptional purity of the ZnO-NPs produced through green synthesis. Through analysing the intensity of absorbance peaks and the wavelength of maximum absorbance (λ_{max}) in the UV-vis spectra of nanoparticles, one can deduce variations in particle size and bandgap energy. The UV-vis spectra showed unique peak shapes and widths, indicating differences in chemical interactions and nanoparticle structures. Changes in wavelength indicate modifications in the electrical structure or surrounding conditions of the nanoparticles, while blue shifts represent transitions to higher energy levels. However, prior research has demonstrated that concentration, temperature, pH, nanoparticle size and shape, and surface plasmon resonance (SPR) bands are all influenced by a variety of factors.

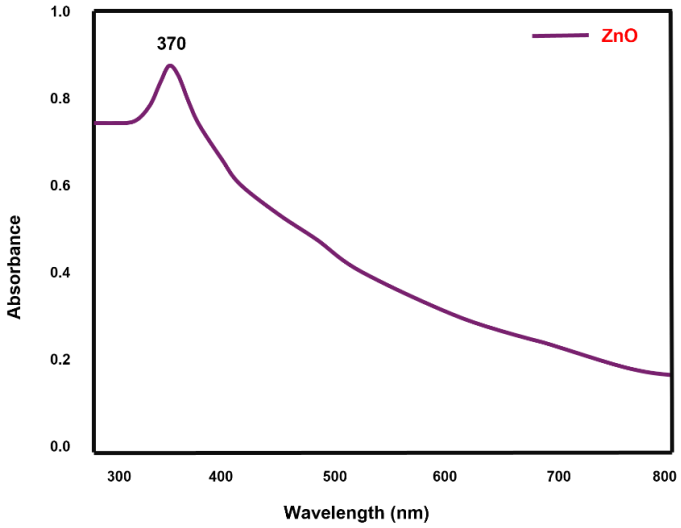

Fig. 1. UV spectra of green synthesized ZnO-NPs

Effect of pH

In order to examine the effect of pH, which is one of the primary factors that affects the formation of nanoparticles, the plant extract (10 mL), zinc acetate (0.02M), and ambient temperature were maintained at the same level.

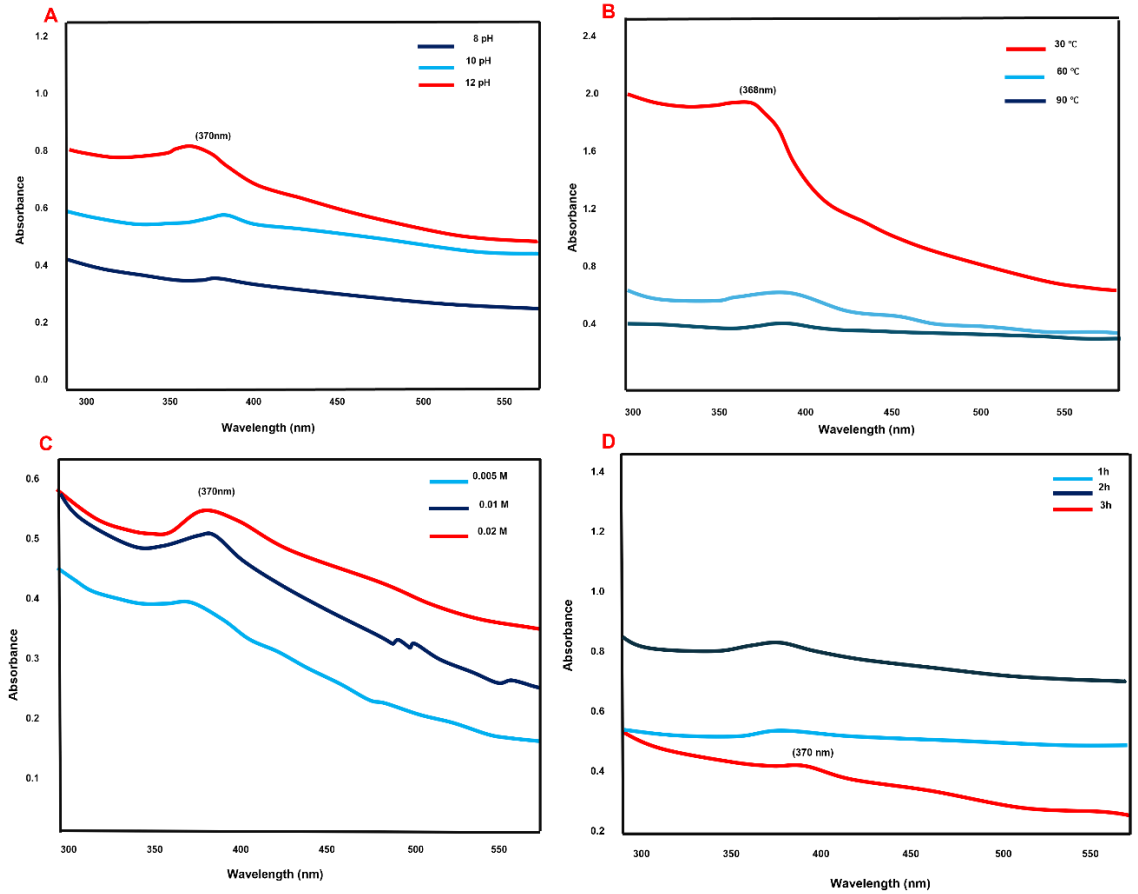

Fig. 2. Absorbance spectra of ZnO NPs obtained: (A) at different pH values of the reaction mixture using plant extract; (B) At different Molarity of zinc acetate; (C) at different time intervals of reaction time; (D) At different reaction temperatures using biosynthesized ZnO NPs

A characteristic absorbance peak for ZnO Nps was observed at 370 nm at pH 12 (Fig. 2A). At pH levels of 8 and 10 no absorbance peaks were observed. This implies that ($Zn(CH_3COO)_2•2H_2O$) was converted to ZnO NPs at pH 12, which suggests the reduction and synthesis of metal oxides.

Effect of metal ion concentration

The concentration of ($Zn(CH_3COO)_2•2H_2O$) also influences the synthesis of nanoparticles, with higher concentrations resulting in increased nanoparticle formation. Nanoparticle synthesis was evaluated at a variety of concentrations (0.005, 0.01, and 0.02 M) in this investigation. The effect of concentration on the absorbance peak was convincingly depicted by the findings. Absorbance peaks were not found at concentrations of 0.005 and 0.01M (Fig. 2B). Nevertheless, an absorbance peak was observed at 0.02 M, as confirmed by UV-Vis spectroscopy, indicating that the concentration had an effect on the formation of ZnO NPs with a characteristic peak at 370 nm.

Effect of reaction time

The reaction time is a critical factor in the synthesis of nanoparticles, as it affects the complete reduction of metal ions, which is dependent upon the type of metal used. The concentrations of *Phyla nodiflora* extract and ($Zn(CH_3COO)_2•2H_2O$) were maintained at a constant level in order to examine the impact of incubation time on nanoparticle formation. The reaction periods were adjusted to 1, 2, and 3 h. The results showed that no absorption peak was observed at 1h (Fig. 2C), but an absorbance peak at 370 nm was detected at 3h. The formation of nanoparticles may be impeded by variations in reaction time (Kalaiselvi *et al.* 2016).

Effect of temperature

To assess the effect of temperature, which is an important factor in nanoparticle synthesis all other parameters were held constant at their respective values. However, at 30 °C, an absorbance peak was observed at 368 nm, which suggested that ($Zn(CH_3COO)_2•2H_2O$) was converted into ZnO NPs (Fig. 2D). Furthermore, no absorbance peaks were observed when the temperature was increased to 60 and 90 °C (Sundaraselvan and Quine 2017).

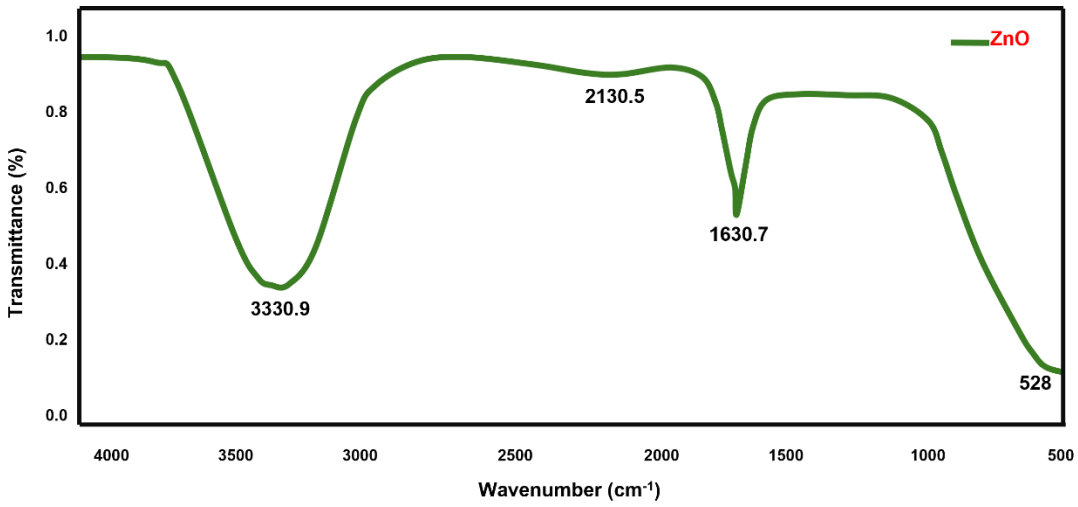

Fig. 3. FTIR spectra of ZnO-NPs

FTIR spectroscopy

Figure 3 depicts the FTIR spectra of ZnO-NPs, emphasizing the essential function of biomolecules from the plant extract in stabilizing and decreasing the biosynthesized ZnO-NPs. The FTIR study detected peaks at 3330.9, 2130.5, 1630.7, and 528 cm^{-1}. The peak at 3330.9 cm^{-1} specifies the stretching vibrations of the O-H group, suggesting the presence of alcohols or phenolic chemicals. The signal at 1630.7 cm^{-1} indicates the presence of carbonyl groups (C=O) and primary amines, whereas the peak at 2130.5 cm^{-1} suggests the presence of alkyne (C≡C) and nitrile (C≡N) groups. The prominent peak at 528 cm^{-1} in the FTIR spectrum verified the production of pure ZnO (Razavian *et al.* 2014). This spectrum analysis offers understanding of the chemical interactions and bonding that influence the creation and durability of the produced nanoparticles.

XRD analysis

The formation of biosynthesized ZnO-NPs was also confirmed by XRD analysis, as shown in Fig. 4. ZnO-NPs structure was confirmed as crystalline hexagonal wurtzite. The XRD spectrum displayed several well-defined diffraction peaks at specific angles: 31.5, 34.2, 36.0, 47.3, 56.4, 62.7, 67.8, 68.7, and 76.7°. The peaks correspond to the Miller indices (110), (002), (101), (102), (110), (103), (112), (201), and (202), respectively (Hasan *et al.* 2019). The synthesized nanoparticles were found to have a hexagonal wurtzite structure, verifying their crystallinity and phase purity of the ZnO NPs by comparing their values to the standard JCPDS Card No. 36-1451.

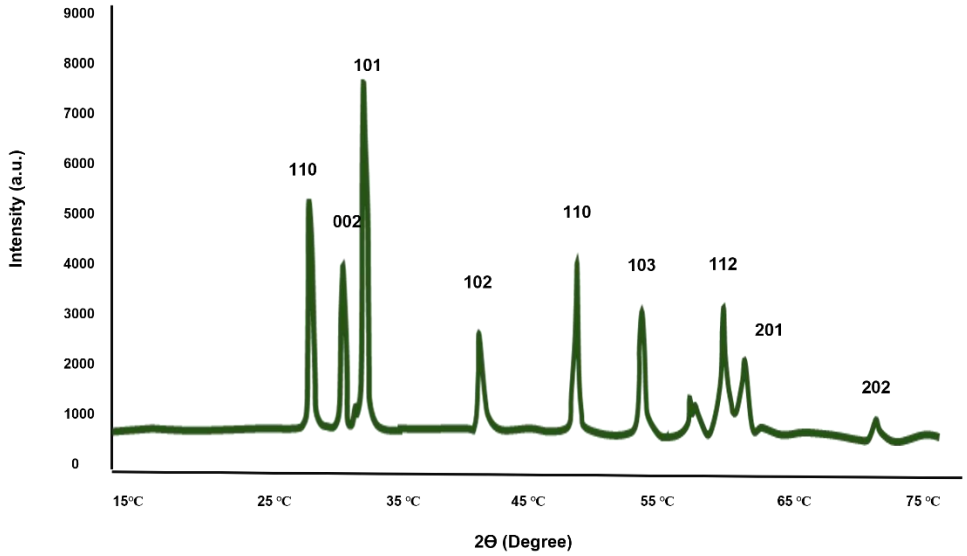

Fig. 4. XRD pattern of ZnO-NPs

TEM analysis

The TEM method was used to study the size and shape of the ZnO-NPs produced through biological synthesis. The TEM pictures showed that the ZnO-NPs had different shapes, such as spheres and hexagonal plates, and were highly clustered with a rugged and uneven surface texture. However, most of the nanoparticles produced with *Phyla nodiflora* extract had sizes ranging from 20 to 50 nm (Figs. 5A and 5B).

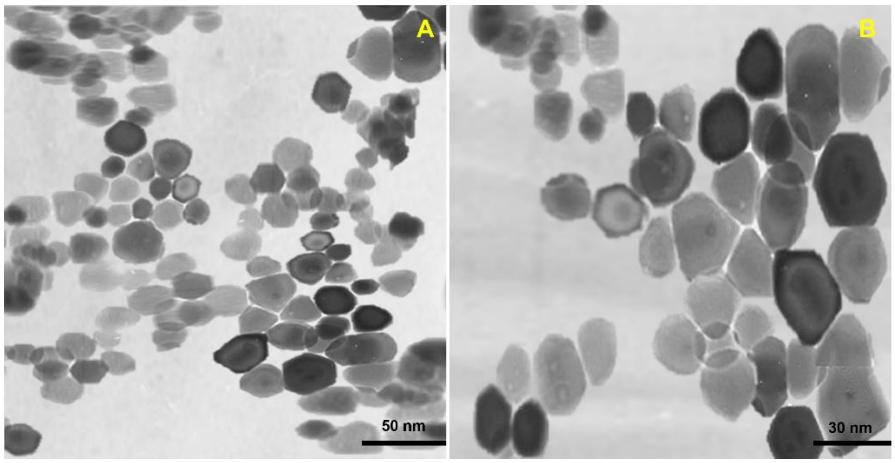

Fig. 5. (A and B) TEM images of produced ZnO-NPs

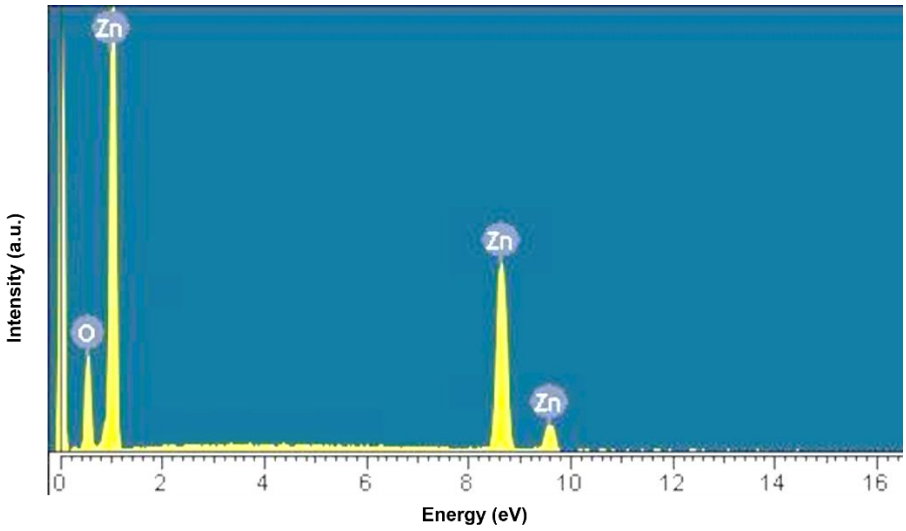

Fig. 6. Energy-dispersive X-ray spectroscopy pattern of synthesized ZnO-NPs

EDX spectroscopy

The EDX method was used to analyze the elemental composition of the ZnO-NPs, with results shown in Fig. 6. The examination verified the quality of the ZnO-NPs by identifying two prominent peaks from 0 to 2 keV representing zinc and oxygen, as well as additional zinc peaks between 8 and 10 keV. The weight and atomic percentages of zinc and oxygen, as shown by the EDX analysis results, are also presented in Fig. 6.

DLS analysis

The DLS analysis was used to determine the particle size distribution, showing an average particle size of 38 nm (Fig. 7A). Biological capping agents, including proteins and enzymes from plant extracts, can affect nanoparticle size by stabilizing them and inhibiting aggregation. However, the particle size distribution of NPs was influenced by a variety of parameters. The results were also compared to the variations in DLS data and the peaks obtained from UV analysis. DLS data verified that the size of nanoparticles was pH-dependent, as they were synthesized at pH levels of 8, 10, and 12. As shown in Table 3 the smallest nanoparticle size (38 nm) was attained at pH 12, while 355 nm and 152 nm were observed at pH 8, 10 respectively. Similarly, nanoparticles of differing sizes were

generated at temperatures of 60 and 90 °C. According to the DLS data, the size of nanoparticles was influenced by temperature, with a size of 105 nm at 60 °C and 356 nm at 90 °C (Table 3). Furthermore, the DLS results demonstrated that the size of the nanoparticles was influenced by the concentration of metal ions, as distinct diameters were observed at concentrations with a size of 160 nm at 0.005 M and with a size of 132 nm at 0.01M.

ZnO-NPs stability was evaluated using zeta potential tests, indicating the zeta potential of the nanoparticles. The observed zeta potential value of -30.3 mV indicates a high level of stability in the solution, as depicted in Fig. 7B. This stability is important for the possible use of these nanoparticles in several domains, such as medicine and environmental cleanup.

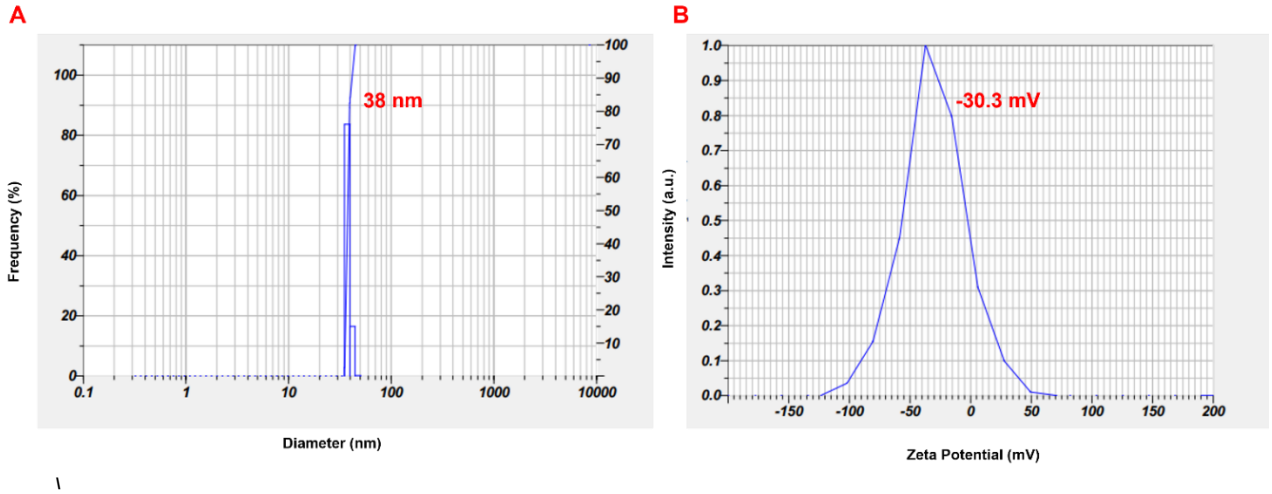

Fig. 7. ZnO-NPs DLS analysis **(A)** and Zeta potential **(B)**

Table 3. Particle Size Variation at Optimum Parameters Confirmed by DLS Analysis of ZnO-NPs

S.no	pH value	Concentration	Temperature	Reaction time	Size (DLS)
1	8	0.02 M	30 °C	3h	355 nm
2	10	0.02 M	30 °C	3h	152 nm
3	12	0.02 M	30 °C	3h	38 nm
4	12	0.01 M	30 °C	3h	132 nm
5	12	0.005 M	30 °C	3h	160 nm
6	12	0.02 M	60 °C	3h	105 nm
7	12	0.02 M	90 °C	3h	356 nm

Biochemical Analysis of Blood Samples

After three weeks, blood samples were biochemically analysed using known procedures to assess renal function and liver enzyme levels.

Assessment of kidney function

The renal function assessment showed that all treated groups experienced a notable decrease in blood uric acid levels. This reduction indicates the good management of high levels of uric acid in the blood and the efficient treatment of gout. The groups treated with ZnO NPs exhibited decreased levels of blood urea and creatinine, as illustrated in Fig. 8. These findings indicated that ZnO NPs have the potential to treat gout in rodents that have been induced by hyperuricemia at lower concentrations. On the other hand, the toxicity and bioaccumulation of AuNPs in mice were investigated in a study that administered varying concentrations of 12.5 nm AuNPs (40, 200, and 400 µg/kg/day) for 8 days (Lasagna-Reeves *et al* 2010), which showed no significant differences in blood urea, uric acid, or creatinine levels between the experimental and control groups. These findings suggest that AuNPs did not cause any toxicity.

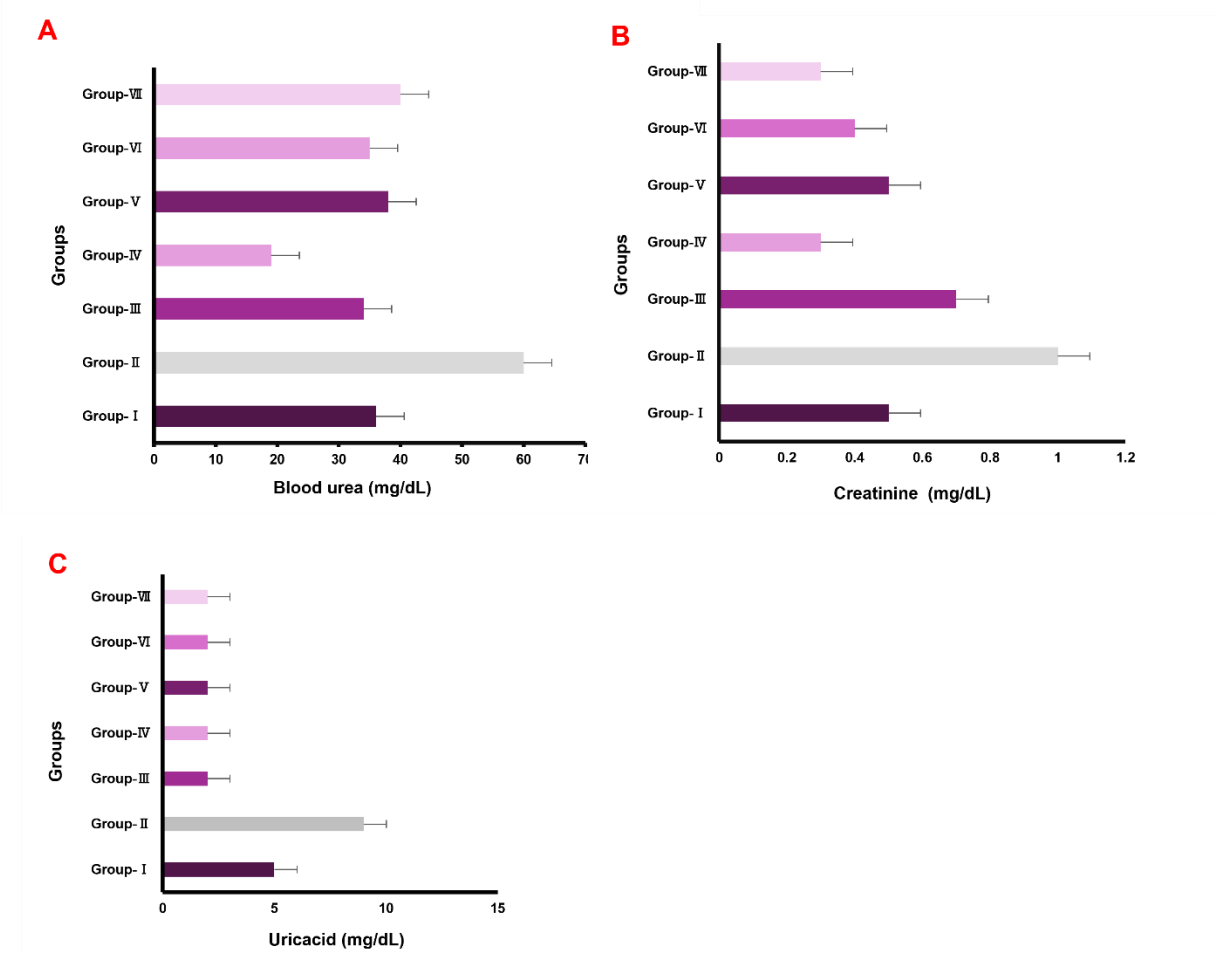

Fig. 8. Test results of kidney: **(A)** Blood urea, **(B)** Creatinine, and **(C)** Uric acid

Liver function test

Group VI showed slightly higher amounts of ALP in the liver function tests compared to a standard mouse. Furthermore, all groups had elevated ALT levels, suggesting liver inflammation in comparison to the baseline levels of normal mice. Elevated levels of AST were seen in Groups II, IV, V, and VI in comparison to normal mice, indicating changes in liver function. Figure 9 displays the comprehensive findings of the liver function tests for each group. On the other hand, the previously conducted research

on the biocompatibility of magnetic iron oxide nanoparticles (Jain *et al.* 2008) in rodents demonstrated alterations in blood serum and tissue over a three-week period following their administration. Within 24 hours, a transient increase in AST, ALT, and ALP was observed, with no long-term effect on liver enzymes or oxidative stress. Similarly, ZnO NPs were orally administered at variable concentrations for a period of three weeks in this experiment. AST, ALT, and ALP levels in blood serum exhibited modest increases by the conclusion of the experiment.

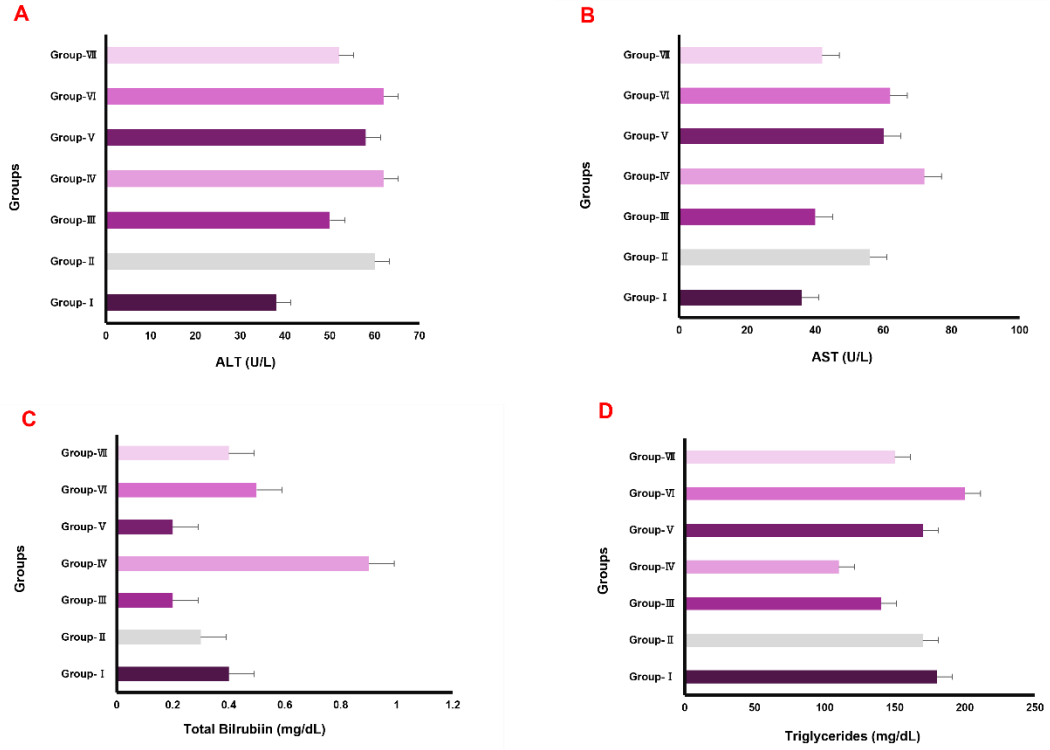

Fig. 9. Test results of liver function **(A)** ALT **(B)** AST (C) total Bilurubin **(D)** ALP

Analysis of lipid profile

Analysis of lipid profiles showed decreased levels of LDL and cholesterol in groups receiving 10 and 20 ppm of ZnO NPs compared to other treated groups. Contrastingly, the groups given allopurinol (50 and 100 mg/kg) showed elevated triglyceride levels, as shown in Fig. 10. Furthermore, prior investigations regarding the ingestion of Ag NPs in rodents demonstrated modifications in blood biochemistry (Razavian *et al* 2014). Over the course of six months, Ag NPs were administered at concentrations of 5, 20, 35, 65, and 95 ppm. The results showed a decrease in cholesterol levels, although the decrease was not statistically significant in comparison to the control. Additionally, the 35 ppm group exhibited a significant reduction in triglycerides.

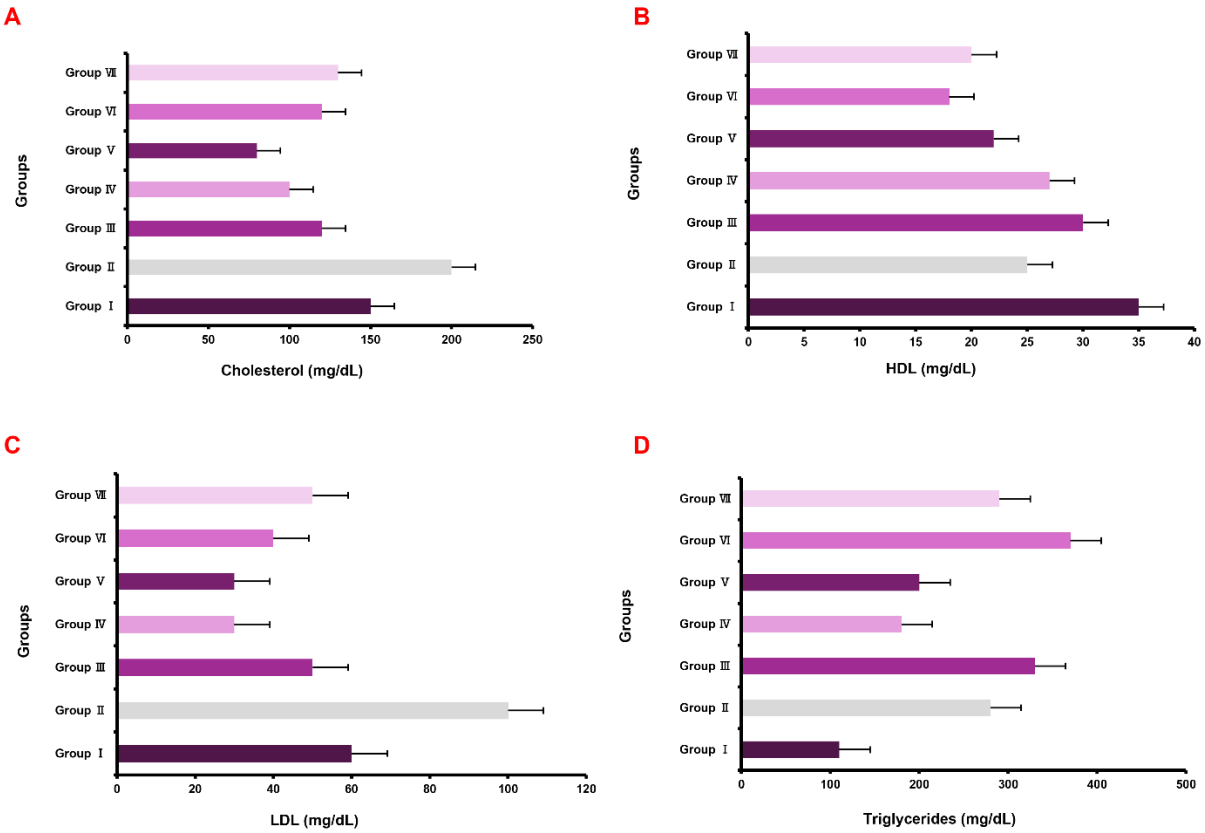

Fig. 10. Lipid profile results: **(A)** Cholesterol**, (B)** HDL, **(C)** LDL**,** and **(D)** Triglycerides

CONCLUSIONS

The study demonstrated an efficient method to produce ZnO-NPs using the phylanodiflora plant. The biofabricated ZnO-NPs were analyzed using advanced methods such as UV-vis, FTIR, TEM, EDX, XRD, and DLS.

1. The UV−vis spectroscopy displayed a distinct peak at 370 nm. The XRD spectrum indicated the wurtzite hexagonal structure of ZnO-NPs. The TEM study revealed that the size of the ZnO-NPs ranged from 20 to 50 nm.
2. ZnO-NPs at lower concentrations could be an efficient treatment for gouty arthritis in mice models. ZnO-NPs delivery at 5, 10, and 20 ppm concentrations showed positive benefits on renal function tests, suggesting their potential use in treating gout.
3. A reduction in blood cholesterol levels was noted in the mice treated with ZnO-NPs, although there were minor changes. A slight elevation in liver function tests (LFTs) was observed in the mice subjects, but it did not result in any significant harm or death.
4. Examinations of liver, muscle, and renal tissues showed no signs of toxicity, indicating the safety of ZnO-NPs at these levels.
5. ZnO-NPs, at low concentrations, demonstrate potential as a non-toxic therapy for gouty arthritis. Nevertheless, the promise of nanoparticles in treating gout justifies additional investigation. Future research should further explore the therapeutic uses of nanoparticles to comprehensively assess their effectiveness and safety in treating gout.

AUTHOR STATEMENTS

Data Availability

The data associated with the findings of this study are available from the corresponding authors, upon reasonable request.

Ethical Approval Statement

The research carried out in this article with animals was in line with the principles and standards outlined in the institutional animal ethical committee of Central South University, Changde city, Hunan Province. All the animal experiments were conducted according to their guidelines and regulations.

Consent to Participate

No human objects were involved in this study.

REFERENCES CITED

Al-Dhabi, A. N., and Arasu, V. M. (2018). "Environmental-friendly green approach for the production of zinc oxide nanoparticles and their anti-fungal, ovicidal, and larvicidal properties," *Nanomaterials* 8(7), article 500. DOI: 10.3390/nano8070500

Ashiq, K., Latif, A., Ashiq, S., and Sundus, A. (2018). "A systematic review on the prevalence, pathophysiology, diagnosis, management and treatment of gout (2007-2018)," *GSC Biol. Pharm. Sci*. 5, 050–055. DOI: 10.30574/gscbps.2018.5.1.0077

Bustanji, Y., Hudaib, M., Tawaha, K., Mohamunad, M., Almasri, I., Hamed, S., Aburjai, T. A., Assaf, A. M., Issa, A. Y., and Alali, F. Q. (2011). "*In vitro* xanthine oxidase inhibition by selected Jordanian medicinal plants," *Jordan J. Pharm. Sci*. 4, 49–55.

Elahi, M., and Matata, B. (2013). "Significance of the nitrosative-oxidative stress disequilibrium on endothelial dysfunction during cardiac development," *Oxidants Antioxid. Med. Sci*. 2, article 73. DOI: 10.5455/oams.070413.rv.006

Foudi, H., Soukeur, A., Rekhila, G. *et al.* (2023). "Synthesis and characterization of ZnO nanoparticles for antibacterial paints," *Chem. Pap.* 77, 1489-1496. DOI: 10.1007/s11696-022-02565-7

Hasan, M., Zafar, A., Yousaf, M., Gulzar, H., Mehmood, K., Hassan, S. G., Saeed, A., Yousaf, A., Mazher, A., Rongji, D., *et al.* (2019). "Synthesis of loureirin B-loaded nanoliposomes for pharmacokinetics in rat plasma," *ACS Omega* 4, 6914−6922. DOI: 10.1021/acsomega.9b00119

Jain, T. K., Reddy, M. K., Morales, M. A., Leslie-Pelecky, D. L., and Labhaset war, V. (2008). "Biodistribution, clearance, and biocompatibility of iron oxide magnetic nanoparticles in rats," *Mol. Pharm.* 5, 316-327. DOI: 10.1021/mp7001285 20

Jamdagni, P., Khatri, P., and Rana, J. S. (2016). "Green synthesis of zinc oxide nanoparticles using flower extract of Nyctanthes arbor-tristis and their antifungal activity," *J. King Saud. Univ. Sci*. 30, 168-175. DOI: 10.1016/j.jksus. 2016.10.002

Jones, M. R., Osberg, K. D., Macfarlane, R. J., Langille, M. R., and Mirkin, C. A. (2011). "Templated techniques for the synthesis and assembly of plasmonic nanostructures," *Chem. Rev*. 111(6), 3736-3827. DOI: 10.1021/cr1004452

Kalaiselvi, A., Roopan, S. M., Madhumitha, G., Ramalingam, C., Al-Dhabi, N. A., and Arasu, M. V. (2016). "*Catharanthus roseus*-mediated zinc oxide nanoparticles

against photocatalytic application of phenol red under UV@ 365nm," *Curr. Sci.* 111, 1811-1815. DOI: 10.18520/cs/v111/i11/1811-1815

Kim, S. Y., Yoo, D. M., Kim, J. H., Kwon, M. J., Kim J.-H., Lee, J. W., Bang, W. J., and Choi, H. G. (2022). "The occurrence of nephrolithiasis in gout patients: A longitudinal follow-up study using a national health screening cohort," *Life* 12(5), article 653. DOI: 10.3390/life12050653

Kuo, C. F., Grainge, M. J., Zhang, W., and Doherty, M. (2015). "Global epidemiology of gout: Prevalence, incidence and risk factors," *Nat. Rev. Rheumatol.* 11, 649-652. DOI: 10.1038/s41584-020-0441-1

Lasagna-Reeves, C., Gonzalez-Romero, D., Barria, M. A., Olimedo, I., Clos, A., Ramanujam, V. M. S., Urayama, A., Vergara, M., Kogan, M. J., and Soto, C. (2010). "Bioaccumulation and toxicity of gold nanoparticles after repeated administration in mice," *Biochem. Biophys. Res. Commun.* 393, 649-655. DOI: 10.1016/j.bbrc.2010.02.046

Matei, A., Cernica, I., Cadar, O., Roman, C., and Schiopu, V. (2008). "Synthesis and characterization of ZnO − polymer nanocomposites," *Int. J. Mater. Form*. 1, 767-770. DOI: 10.1007/s12289-008-0288-5

Razavian, M. H., and Masaimanesh, M. (2014). "Ingestion of silver nanoparticles leads to changes in blood parameters," *Nanomed. J.* 1, 339-345. DOI: 10.7508/NMJ.2015.05.008

Razavian, M. H., and Masaimanesh, M. (2014). "Ingestion of silver nanoparticles leads to changes in blood parameters," *Nanomed. J.* 1, 339-345

Richette, P., Perez-Ruiz, F., Doherty, M., Jansen, T. L., Nuki, G., Pascual, E., Leonardo, P., So, A. K., and Bardin, T. (2014). "Improving cardiovascular and renal outcomes in gout: What should we target?" *Nat. Rev. Rheumatol*. 10, 654-661. DOI: 10.1038/nrrheum.2014.124

Sajid, M. M., Shad, N. A., Javed, Y. *et al.* (2022). "Efficient photocatalytic and antimicrobial behaviour of zinc oxide nanoplates prepared by hydrothermal method," *J. Clust. Sci.* 33, 773-783. DOI: 10.1007/s10876-021-02013-8

Sezai, A., Soma, M., Nakata, K., Hata, M., Yoshitake, I., Wakui, S., Shiono, M., and Yaoita, H. (2015). "Comparison of febuxostat and allopurinol for hyperuricemia in cardiac surgery patients with chronic kidney disease (NU-FLASH Trial)," *J. Cardiol*. 66, 298-303. DOI: 10.1016/j.jjcc.2014.12.017

Singh, P., Kim, Y. J., Zhang, D., and Yang, D. C. (2016). "Biological synthesis of nanoparticles from plants and microorganisms," *Trends. Biotechnol*. 34, 588-599. DOI: 10.1016/j.tibtech.2016.02.006

Slavin, Y. N., Asnis, J., Häfeli, U. O., and Bach, H. (2017). "Metal nanoparticles: Understanding the mechanisms behind antibacterial activity," *J. Nanobiotechnol*. 15, 1-20. DOI: 10.1186/s12951-017-0308-z

So, A., De Smedt, T., Revaz, S., and Tschopp, J. (2007). "A pilot study of IL-1 inhibition by anakinra in acute gout," *Arthritis Research & Therapy* 9(2), R28. DOI: 10.1186/ar2143

Susyani, S., and Desvianti, D. (2017). "Nutrition counseling among patients with gout," *Int. J. Publ. Health Sci*. 6(4), 360-370. DOI: 10.11591/ijphs.v6i4.10784

Sundaraselvan, S., and Quine, S. D. (2017). "Green synthesis of zinc oxide nanoparticles using seed extract of *Murraya koenigii* and their antimicrobial activity against some human pathogens," *J. Nanosci. Tech.* 3, 289-292

Wang, L., Hu, C., and Shao, L. (2017). "The antimicrobial activity of nanoparticles: Present situation and prospects for the future," *Int. J. Nanomed*. 12, 1227-1249. DOI: 10.2147/ijn.s121956

Zare, E., Pourseyedi, S., Khatami, M., and Darezereshki, E. (2017). "Simple biosynthesis of zinc oxide nanoparticles using nature's source, and it's in vitro bio-activity," *Journal of Molecular Structure* 1146, 96-103. DOI: 10.1016/j.molstruc.2017.05.118

Zhang, W., Iso, H., Murakaini, Y., Miura, K., Nagai, M., Sugiyaina, D., Ueshina, H., and Okamura, T. (2016). "Serum uric acid and mortality form cardiovascular disease: EPOCH-JAPAN study," *J. Atheroscler. Thromb*. 23, 692-693. DOI: 10.5551/jat.31591

Article submitted: June 23, 2024; Peer review completed: August 17, 2024; Revised version received and accepted: September 28, 2024; Published: October 28, 2024.
DOI: 10.15376/biores.19.4.9544-9559